The Influence of Metal Plates on Quench Protection of High Temperature Superconducting Pancake Coils

Zhen Lu, Yawei Wang, Qingqing Yang, Wenbo Xue, Yutong Fu, Binyu Huang, Zhiyong Hong, and Zhijian Jin

The Influence of Metal Plates on Quench Protection of High Temperature Superconducting Pancake Coils

Zhen Lu, Yawei Wang, Qingqing Yang, Wenbo Xue, Yutong Fu, Binyu Huang, Zhiyong Hong, Zhijian Jin

Abstract—**Quench has always been an urgent problem for high temperature superconductor (HTS) magnets. Fast discharge of the coil current is an effective method to protect the HTS magnet from quenching. In HTS magnets, metal plates are originally used to provide conduction cooling and mechanical support for the coil. During fast discharging operations, the metal plates can rapidly absorb part of the magnetic energy stored in the HTS coils through electromagnetic coupling. Previous studies are based on copper plates. This paper studies the influence of several promising metal materials on the discharging process of the HTS coils coupled with metal plates by experiments and simulations. The results show that in the explored resistance range, the higher the electrical conductivity of the metal plates, the better the acceleration of the current attenuation of coil at the early stage of discharging process. The effects of different metal plates on accelerating current attenuation of the coil are ranked as follows: SS 304L < Al 6061-T6 < Al (RRR = 30) < Cu (RRR = 30) < Au < Cu (RRR = 300) < Ag. However, Cu (RRR = 300) plates can absorb more energy from the HTS coil than the Ag plates during the discharging process. Copper with higher purity (Cu (RRR = 300)) and silver are promising alternatives for metal plates of HTS magnets. Generally, a fast current drop is always the most effective method for avoiding tape turn-out during a local quench; therefore, silver with the highest electrical conductivity is the best choice in view of quench protection.**

Index Terms—**HTS coil, Quench protection, Fast discharge, Metal plate.**

I. INTRODUCTION

HIGH temperature superconducting (HTS) magnets often operate at high magnetic fields and high current densities, and store enormous magnetic energy [1], [2]. Thus, overheating damage caused by quenching has always been a great challenge for HTS high-field magnets [3], [4]. The quench propagation in HTS coils is slow; thus, it is difficult to detect a local hot-spot-induced quench at its early stage [5]-[8]. Massive joule heat can be generated at local quench zones, resulting in a high hot-spot temperature in the HTS coils. The operating current of the HTS magnet must be discharged before the hot-spot temperature exceeds the safety limit [9]. Therefore, fast discharge is key for successful quench protection of HTS magnets.

A basic active quench protection system promptly forces the energy stored in the coil to be released using dump resistances or quench heaters [10]-[13]. However, an excessively fast discharging operation may lead to voltage breakdown in the coil [14], [15]. It is sometimes difficult for the quench heater to heat the entire HTS coil to the normal state in a sufficiently short time when the coils are too large [16], [17]. Metal plates are typically used in superconducting magnets for mechanical support and conduction cooling. During fast discharge operations with dump resistances, a considerable part of the magnetic energy stored in the HTS coils can be transmitted into metal plates through electromagnetic coupling [18], [19]. This can accelerate not only the discharge of the coil, but also the coil heating process. This has been proposed and studied based on copper plates [20], [21]. However, a variety of metal materials, such as copper, brass, aluminum alloy, and stainless steel, are promising alternatives for this technique.

A HTS magnet (25 T @4.2 K) with 12 double pancake coils is being developed at Shanghai Jiao Tong University, which is an industry-scale quench test magnet for compact Tokamak HTS magnets. This study investigates the influence of metal materials on the discharging behavior of HTS coils coupled with metal plates. First, the influence of copper and brass plates is analyzed by measurements on a small HTS test coil. Then, a simulation study is performed on an industry-scale HTS double pancake coil, which is for the 25 T @4.2 K HTS magnet. Several different metal materials are analyzed: stainless steel 304L, Al 6061-T6, Ag, Au, Al (RRR = 30), Cu (RRR = 30), and Cu (RRR = 300). The influence of different metal plates on accelerating the discharge of the HTS coil is studied by comparing the coil current, integral of the square current, current in the metal plates, and temperature rise of the coil and metal plates.

II. EXPERIMENT

A. Experiment setup

The experimental platform is shown in Fig. 1. The coil used for testing is a double pancake (DP) coil wound using second-generation HTS ReBCO tapes. The tape is wrapped with Kap-

ton strips. The specifications of the coils are listed in Table I. The coil frame is made of G10, and no metallic materials are used in the coil frame to eliminate electromagnetic interference. A copper plate and brass plate are prepared for the experiment, and the two plates are of the same size. The thickness of both plates is 1 mm, and the inner and outer diameters are 70 mm and 120 mm, respectively. The metal plates are wrapped with Kapton sheet as electrical insulation. The coil and metal plates are immersed in liquid nitrogen (77 K) during the discharge tests. The positions of the HTS coil and plates used in the tests are shown in Fig. 1(a).

In the experiments, first, the coil is ramped up to an expected transport current by a DC power supply, and then, the metal plate is placed coaxially with the coil. After the coil and metal plate are cooled to a stable state, a discharging test with dump resistance is performed on the HTS coil. The current and voltage of the coil are measured using an oscilloscope in the process. Three discharging tests are performed on the HTS coil: without metal plate, with a brass plate, and with a copper plate.

TABLE I
SPECIFICATIONS OF TEST COIL AND INDUSTRY-SCALE COIL

| Parameters	Test coil	Industry-scale coil
Tape width/thickness	4/0.25 mm	10 mm/ 95.3 μm
Average thickness of each turn	444 μm	120.3 μm
Number of turns, DP	27×2	450×2
Inner/outer diameter	80/104 mm	100/208 mm
Turn-to-turn insulation	Kapton	Kapton
Field per Ampere at center	0.736 mT/A	7.43 mT/A
Self-inductance	0.4 mH	127.7 mH
Distance between upper and lower coils	0.4 mm	1 mm
Critical current of the coil	96 A, @77 K	1351 A, @4.2 K
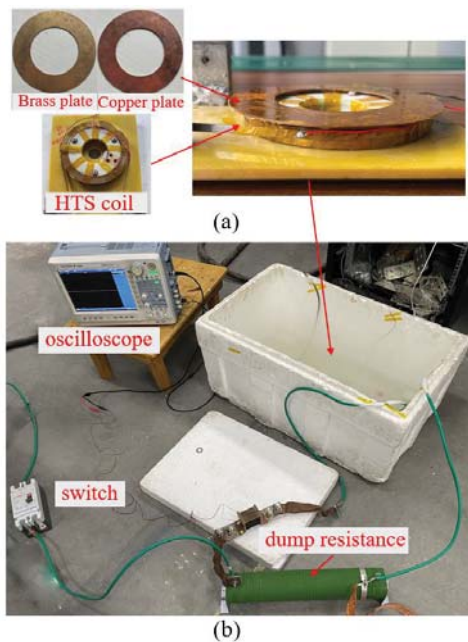
Fig. 1. Experiment setup for discharging tests of the HTS double pancake coil: (a) The position of the HTS coil and plate; (b) Experimental circuit diagram.

B. Experiment results
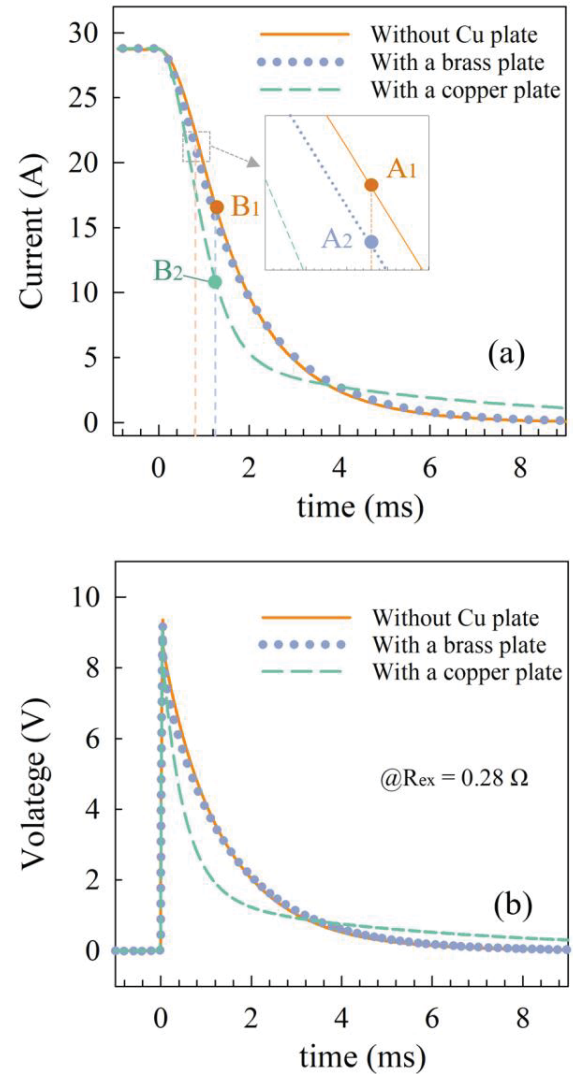
Fig. 2. Discharging process of the coil with different metal plates when dump resistance is 0.28 Ω: (a) current in the coil; (b) Voltage across the coil. Note that A_1 and B_1 are points on the solid line, point A_2 is on the dotted line, and point B_2 is on the dashed line.

The current and voltage of the measured coil are shown in Fig. 2. The external dump resistance R_{ex} is 0.28 Ω, and the initial transport current is 28.8 A, which is 30 % of the critical current of the HTS coil. The beginning of the discharging process is $t = 0$. A high coil voltage is generated suddenly at the beginning of the discharging process, and then the coil voltage decays gradually to zero. Compared with the discharging test without metal plates, the test with the brass plate has the largest current difference at $t = 0.86$ ms. The current of the coil without the plate at this time is 21.61 A, which is at point A_1; the current of the coil with the brass plate at this time is 20.45 A, which is at point A_2. The difference is only 4.03 % of the initial transport current, 28.8 A. The case with the copper plate shows a much faster current drop, and the maximum difference occurs at $t = 1.3$ ms, and the maximum current difference

is 5.84 A, 20.28 % of the initial transport current, which is five times that of the brass plate.

The measurements show that the coupled copper plate can significantly accelerate the discharging process of the HTS coil at its early stage, which matches well with the previous studies in [21]. However, the coupled brass plate shows less effect on the discharging process, although it also speeds up the discharging process to some extent. At 77 K, the resistivity of the copper used in the experiment is 2.51×10^{-9} Ω·m, and the resistivity of the brass used is 4.66×10^{-8} Ω·m, which is an order of magnitude higher than that of copper. Therefore, there is no considerable current induced in the brass plate.

III. MODEL AND STUDY CASE

A. Model development

A 2D axisymmetric multi-physics model is developed for this study, which couples a magnetic field module with A-formulation, a heat transfer module, and a circuit network module. The relationship between the three modules is shown in Fig. 3. The magnetic field and heat transfer modules are solved by the finite element method, and both FEM modules and the circuit network module are built in COMSOL. The circuit module calculates the current variation in the HTS coils. The current in the metal plates is assumed to be uniformly distributed, so metal plates can be equivalent to secondary coils for electromagnetic coupling with the HTS coil. This method is introduced in detail in [21]. The magnetic field module is coupled to the circuit network module to calculate the eddy current induced in the metal plates, and the governing equation is:

$$\begin{cases} \nabla \times \mathbf{B} = \mu \mathbf{J} \\ \mathbf{B} = \nabla \times \mathbf{A} \end{cases} \quad (1)$$

where $\mathbf{B}$ and $\mathbf{A}$ are the magnetic flux density and magnetic vector potential, respectively, and μ is the permeability. $\mathbf{J}$ is the external current density, which is calculated using the circuit network module. The heat transfer module is coupled with a magnetic field module through an electromagnetic heating interface to calculate the temperature distribution of the HTS coil and metal plates. The governing equation of the heat transfer module is:

$$\rho C \frac{\partial T}{\partial t} + \nabla \cdot (-k \nabla T) = Q \quad (2)$$

where ρ is the density, k is the thermal conductivity, and C is the heat capacity of the material. Q is the heat source, which is obtained from the eddy current in the metal plates. The temperature distribution of the metal plates is fed back to the circuit network module. The model is validated experimentally by comparing the currents and voltages from the measurements and simulations, as shown in Fig. 4. There is a slight measurement error between the measurements and simulations.
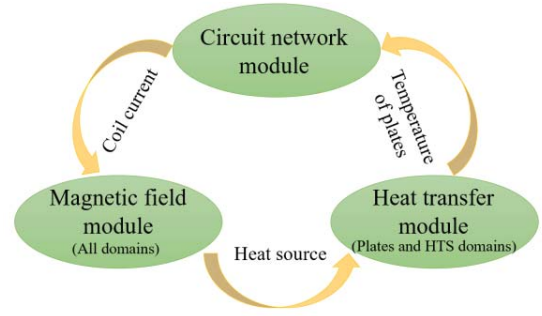
Fig. 3. Coupled modules for the HTS coils with metal plates.
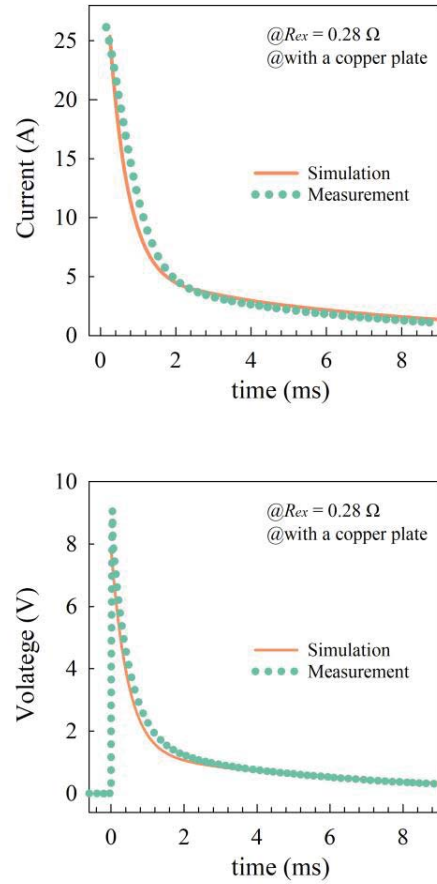
Fig. 4. The current and voltage of the coil from measurement and simulation in the fast discharging process with a dump resistance 0.28 Ω, which is for the test HTS coil in Table I.

B. Studied industry-scale HTS coil

An industry-scale HTS DP coil with a larger size and more turns is studied in this section (25 T all-HTS magnet). The coil comprises ReBCO tapes and is insulated using Kapton tapes. Three identical metal plates are used to provide mechanical support and conduction cooling, as shown in Fig. 5. More details regarding the DP coil are presented in Table I.

In the simulation, a variety of common metal materials are analyzed, including silver (Ag), gold (Au), aluminum (Al (RRR = 30)), copper (Cu (RRR = 30), Cu (RRR = 300)), aluminum alloy 6061-T6, and stainless steel 304L (SS 304L).

The electromagnetic and thermal properties of Ag and Au are obtained from the COMSOL material library. Reference [22] provides the electromagnetic and thermal properties of Al (RRR = 30), Cu (RRR = 30), Cu (RRR = 300), Al 6061-T6, and SS 304L. In this study, the initial operating temperature is 4.2 K, the initial transport current is 300 A, and the dump resistance is 0.5 Ω. The coil current, current in the metal plates, and temperature of the model are analyzed.
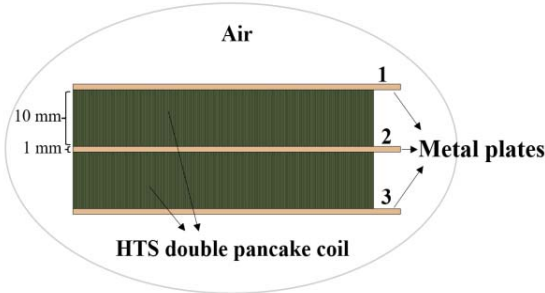

Fig. 5. Schematic illustration of the HTS double pancake coil with metal plates.

IV. RESULTS AND DISCUSSION

A. Coil current

Fig. 6 shows the variation in the coil current during the fast discharging tests. The current of the coil with SS 304L plates is almost the same as the current of the coil without metal plates. In three cases of Au, Cu (RRR = 300), and Ag, the coil current decays with a similar trend, which has a rapid decline at first, followed by a rebound and then decays gradually to zero. The coil with Ag plates shows the fastest current drop at the early stage, which is up to 95 % of the initial current at $t = 50$ ms. Its rebound is also the highest, which is 30.6 % of the initial current at $t = 404$ ms. Fig. 7 shows the temperature-dependent electrical conductivity of different metal materials in the temperature range of 4–70 K [22]. In the range of 4–10 K, the resistivities of SS 304L and aluminum alloy 6061-T6 are so high that few currents are generated in the plates; therefore, these two materials have little effect on the discharge process. Ag has the highest electrical conductivity, leading to the most significant acceleration effect on the coil current at an early stage. The higher the electrical conductivity of the material, the lower the coil current drops caused by the metal plates at the early stage of discharge. However, higher electrical conductivity of the metal plates can also lead to a more significant rebound of the coil current in the subsequent stage, which may lead to a second quench of the HTS coil.

A parameter k is defined to represent the influence of metal plates on the discharge of the HTS coil. The equation is as:

$$k = \max \left\{ \frac{\left| I_{no-plate}(t) - I_{with-plate}(t) \right|}{I_0} \right\} \times 100\% \quad (3)$$

where $I_{no-plate}$ and $I_{with-plate}$ represent the discharging current of the coil with and without metal plates, respectively, and I_0 is the initial coil current. The corresponding time of k is de-

fined as t_k. Fig. 8 shows k and t_k for the seven study cases with different metal materials. The maximum current difference between the two cases (with and without metal plates) occurs at t_k, and the maximum difference is k of the initial transport current. As shown in Fig. 8, the higher the electrical conductivity of the material, the larger the k, and k is approximately linearly related to t_k. In the seven cases with different materials, the current of the coil with metal plates decays with a similar rate at the very early stage of the discharging process.

TABLE II
PARAMETERS OF DIFFERENT METAL PLATES

Metal materials	$\int_0^t I^2 dt$	Ratio η
Without plate	11491.3	/
SS 304L	11486.6	99.96 %
Al 6061-T6	11326.6	98.57 %
Al – RRR=30	9350.5	81.37 %
Cu - RRR=30	8471.9	73.72 %
Au	7803.2	67.91 %
Cu – RRR=300	4604.1	40.06 %
Ag	5338.6	46.46 %

The integral of the square current of the coil can estimate the increase in hot spot temperature in the coil during the discharge process [9]. A parameter η is defined to describe the ratio of the integral of the square current of the coil with and without metal plates. The definition of parameter η is as:

$$\eta = \frac{\int_0^t I_{with-plate}^2 dt}{\int_0^t I_{no-plate}^2 dt} \times 100\% \quad (4)$$

where $I_{no-plate}$ and $I_{with-plate}$ represent the discharging current of the coil with and without metal plates, respectively, and t is the discharge time, which is 2 s for all discharging operations. In the discharging process without metal plates, the energy stored in the coil at the initial state is dissipated in the dump resistance. The dump resistance is a constant, so η can also represent the ratio of the energy dissipation in the dump resistance to the total energy. During the discharging process with metal plates, metal plates can absorb energy from the coil through electromagnetic coupling and convert it to joule heat; thus, the total energy is dissipated simultaneously in the metal plates and dump resistance. Therefore, the decrease in η can not only represent the decrease in hot spot temperature in the HTS coil, but also describe the increase in energy dissipation in the metal plates. The η values of the seven different materials are displayed in Table II. Generally, a plate with a lower resistivity can absorb more energy from the HTS coil and its η is lower. The lower η, the more favorable for the quench protection of the HTS coils.

However, η of the Ag plates is slightly higher than that of Cu (RRR = 300) plates, although Ag has a lower resistivity and higher k than Cu (RRR = 300). This is because the electrical conductivity of Ag decays much more significantly with temperature than that of Cu (RRR = 300), and the rebound of

the coil current is much more significant than that of Cu (RRR = 300); thus, the integral of the square current of the coil with Ag plates is higher. During the current rebounding process, the coil absorbs energy from the metal plates, so the energy dissipation in the Ag plates is lower than that in the Cu (RRR = 300) plates.
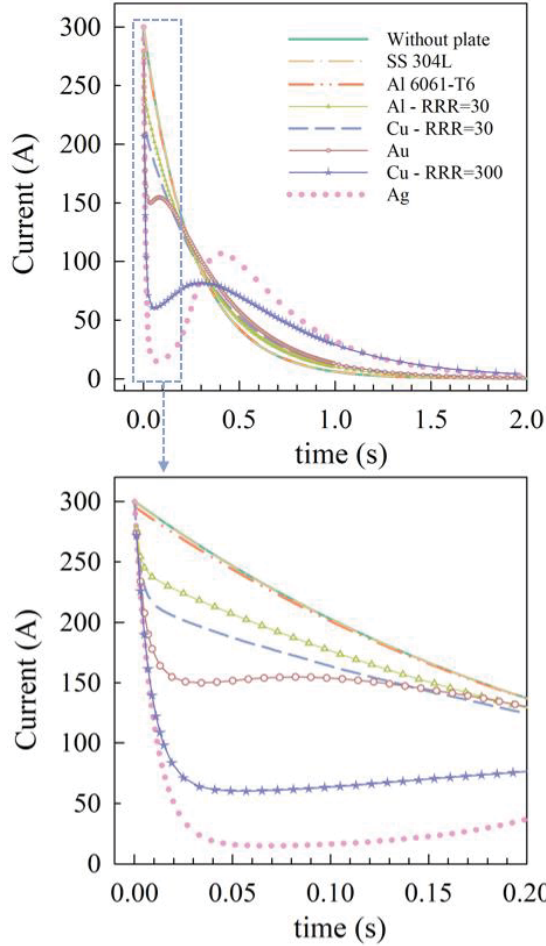

Fig. 6. Current of the coil with different metal plates during fast discharging tests. The dump resistance is 0.5 Ω. Note that the curve of SS 304L basically coincides with the curve "Without plate".
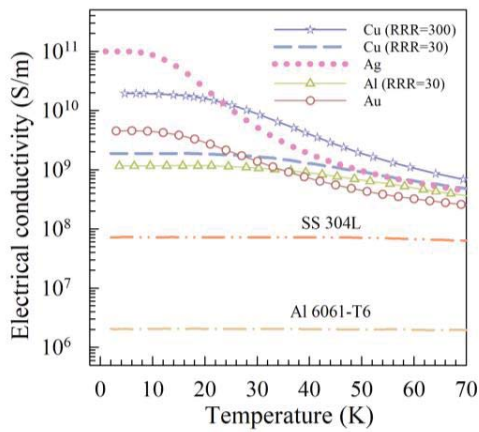

Fig. 7. Temperature-dependent electrical conductivity of different metal materials [22].
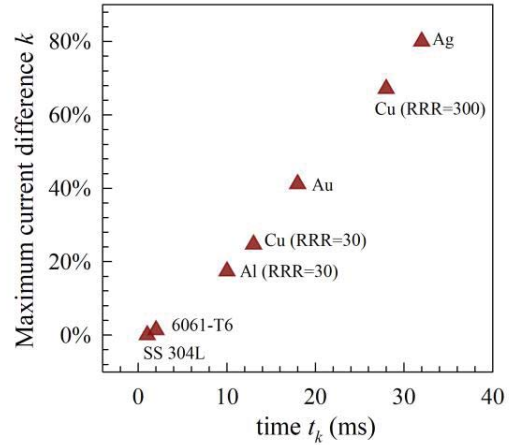
Fig. 8. k and t_k in the seven cases with different metal materials.

B. Current of metal plates

Fig. 9. Current in different metal plates during fast discharging tests: (a) Metal plate 1 or 3; (b) Metal plate 2. The number of metal plates is marked in Fig. 5.

The above results show that Al (RRR = 30), Cu (RRR = 30), and Cu (RRR = 300) are relatively practical materials for metal plates, which can significantly accelerate the discharging process and have an acceptable price. This section uses them

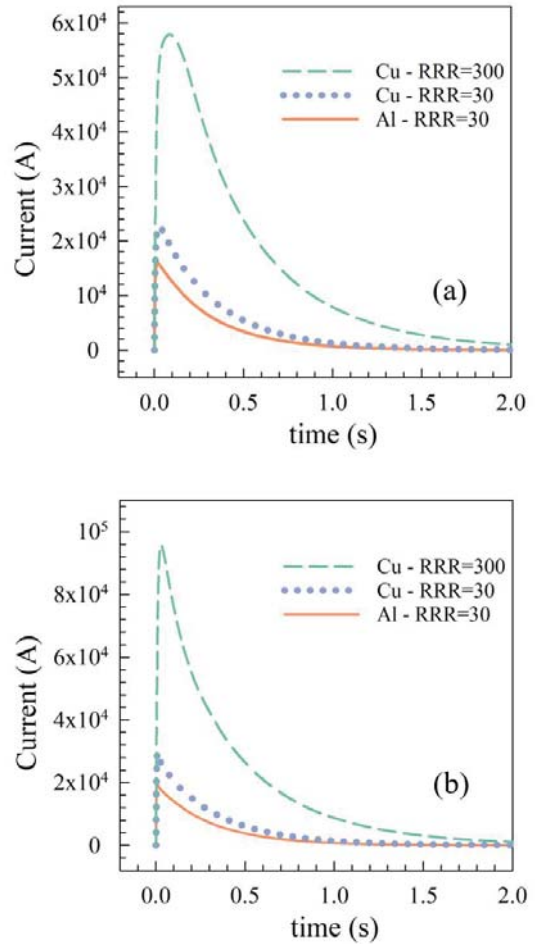as examples to study the variation in their current during fast discharging operations, as shown in Fig. 9. Plates 1 and 3 have the same current variation because of their symmetrical position. The total current induced in the metal plates rises rapidly to a peak at the beginning of the fast discharge process and then gradually decays to zero. As shown in Fig. 7, in the temperature range of 4–10 K, the electrical conductivity of Cu (RRR = 300) is one order of magnitude larger than that of Cu (RRR = 30), thus the peak current of Cu (RRR = 300) plates is much higher than that of the Cu (RRR = 30) plates. Al (RRR = 30) has the lowest conductivity, leading to the lowest induced current peak in the plates.

C. Temperature of metal plates and HTS coil.

Fig. 10 shows the average temperature of the metal plates and HTS coil during the fast discharging operations. During the entire discharge process, the maximum temperature difference of the HTS coil with metal plates is less than 2 K, thus the whole coil is uniformly heated by the metal plates. In the case of Cu (RRR = 300), the temperature rise is 35.1 K, which is 37.6 % higher than that of Cu (RRR = 30). In the case of Al (RRR = 30), the temperature rise is the lowest, only 22.5 K. As shown in Table II, the order of the ratio η of the metal plates during the discharging process is Cu (RRR = 300) < Cu (RRR = 30) < Al (RRR = 30). The heat capacities of Cu (RRR = 300) and Cu (RRR = 30) are the same, slightly lower than that of Al (RRR = 30). Therefore, the lower η and heat capacity of the metal plates, the higher the temperature rise of the model.
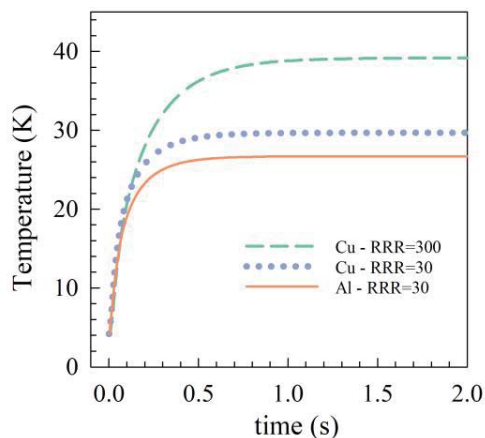

Fig. 10. Average temperature of the metal plates and HTS coil during fast discharging tests.

V. CONCLUSION

In this paper, the influence of different metal plates on the fast discharge of HTS coils is studied through experimentations and simulations. The results show that the effects of different metal plates on accelerating coil current attenuation at the early stage of the discharging process are ranked as follows: SS 304L < Al 6061-T6 < Al (RRR = 30) < Cu (RRR = 30) < Au < Cu (RRR = 300) < Ag. The higher the electrical

conductivity of the metal plates, the better the acceleration of the current attenuation of the coil.

A higher electrical conductivity can lead to more energy being absorbed by the metal plates. However, the more significant the current rebound, the higher the integral of the square current of the coil. Compared with Ag plates, Cu (RRR = 300) plates can absorb more energy and reduce the hot spot temperature in the coil more significantly. Both Cu (RRR = 300) and silver are promising materials for metal plates of HTS coils. Generally, a fast current drop is always the most effective method for avoiding tape turn-out during a local quench; therefore, silver with the highest electrical conductivity is the best choice in view of quench protection.

REFERENCES

[1] S. Hahn et al., "45.5-tesla direct-current magnetic field generated with a high-temperature superconducting magnet," *Nature,* vol. 570, no. 7762, pp. 496-499, Jun 2019.

[2] J. Bascunan, S. Hahn, T. Lecrevisse, J. B. Song, D. Miyagi, and Y. Iwasa, "An 800-MHz all-REBCO Insert for the 1.3-GHz LTS/HTS NMR Magnet Program-A Progress Report," *IEEE Trans. Appl. Supercond.,* vol. 26, no. 4, Jun 2016, Art no. 4300205.

[3] H. H. Song, K. Gagnon, and J. Schwartz, "Quench behavior of conduction-cooled YBa2Cu3O7-delta coated conductor pancake coils stabilized with brass or copper," *Supercond. Sci. Technol.,* vol. 23, no. 6, Jun 2010, Art no. 065021.

[4] Y. Wang, C. Wan Kan, and J. Schwartz, "Self-protection mechanisms in no-insulation (RE)Ba 2Cu 3O x high temperature superconductor pancake coils," *Supercond. Sci. Technol.,* vol. 29, no. 4, April 2016, Art no. 045007.

[5] T. Lecrevisse et al., "Quench Propagation in YBCO Pancake: Experimental and Computational Results," *IEEE Trans. Appl. Supercond.,* vol. 23, no. 3, Jun 2013, Art no. 4601805.

[6] H. H. Song and J. Schwartz, "Stability and Quench Behavior of YBa2Cu3O7-x Coated Conductor at 4.2 K, Self-Field," *IEEE Trans. Appl. Supercond.,* vol. 19, no. 5, pp. 3735-3743, Oct 2009.

[7] R. H. Bellis and Y. Iwasa, "Quench propagation in high Tc superconductors," *Cryogenics,* vol. 34, no. 2, pp. 129-144, 1994.

[8] C. Lacroix, Y. Lapierre, J. Coulombe, and F. Sirois, "High normal zone propagation velocity in second generation high-temperature superconductor coated conductors with a current flow diverter architecture," *Supercond. Sci. Technol.,* vol. 27, no. 5, 2014, Art no. 055013.

[9] E. Haro, A. Stenvall, J. van Nugteren, and G. Kirby, "Hot Spot Temperature in an HTS Coil: Simulations With MIITs and Finite Element Method," *IEEE Trans. Appl. Supercond.,* vol. 25, no. 2, Apr 2015, Art no. 4901107.

[10] M. A. Green and Iop, "Various Quench Protection Methods for HTS Magnets," *Conference Series: Materials Science and Engineering,* 2020, vol. 755, no. 1: IOP Publishing, p. 012134.

[11] K. Wang et al., "Analysis and Design of Fast Discharge Resistor System Based on Forced-Air Cooling Method," *IEEE Trans. Plasma Sci.,* vol. 48, no. 2, pp. 542-553, Feb 2020.

[12] F. Rodriguez-Mateos and F. Sonnemann, "Quench heater studies for the LHC magnets," *PACS2001. Proceedings of the 2001 Particle Accelerator Conference (Cat. No.01CH37268),* vol.5, pp. 3451-3, 2001.

[13] P. D. Noyes et al., "Protection Heater Development for REBCO Coils," *IEEE Trans. Appl. Supercond.,* vol. 22, no. 3, Jun 2012, Art no. 4704204.

[14] K. Wang, Z. Q. Song, P. Fu, W. Tong, H. Li, and X. Q. Zhang, "Structure Optimization of Fast Discharge Resistor System for Quench Protection System," *IEEE Access,* vol. 7, pp. 52122-52131, 2019.

[15] Y. Li et al., "A Passive Quench Protection Design for the 9.4 T MRI Superconducting Magnet," *IEEE Trans. Appl. Supercond.,* vol. 24, no. 3, Jun 2014, Art no. 4401605.

[16] E. Todesco, "Quench limits in the next generation of magnets," *arXiv preprint arXiv*:1401.3931, 2014.

[17] T. Salmi and A. Stenvall, "Modeling Quench Protection Heater Delays in an HTS Coil," *IEEE Trans. Appl. Supercond.,* vol. 25, no. 3, Jun 2015, Art no. 0500205.

[18] H. H. Song, "Sudden-Discharge Cycling Characteristics and Millisecond Dynamic Behaviors of a HTS Stainless-Steel Insulated Double-Pancake Coil With Thin Copper Plates," *IEEE Trans. Appl. Supercond.,* vol. 30, no. 4, Jun 2020, Art no. 4702506.

[19] P. Fazilleau, F. Borgnolutti, and T. Lecrevisse, "Protection Design for a 10-T HTS Insert Magnet," *IEEE Trans. Appl. Supercond.,* vol. 26, no. 3, Apr 2016, Art no. 4700705.

[20] R. Gupta et al., "High field HTS solenoid for a muon collider—Demonstrations, challenges, and strategies," *IEEE Trans. Appl. Supercond.,* vol. 24, no. 3, June 2014, Art no. 4301705.

[21] H. Witte, W. B. Sampson, R. Weggel, R. Palmer, and R. Gupta, "Reduction of the Hot Spot Temperature in HTS Coils," *IEEE Trans. Appl. Supercond.,* vol. 24, no. 3, Jun 2014, Art no. 4601904.

[22] P. Duthil, "Material properties at low temperature," *arXiv preprint arXiv:*1501.07100, 2015.